When Asymmetry Helps: Joint Power and Blocklength Optimization for Non-Orthogonal Multiple Access in Downlink Communications

Haïfa Farès, Rémi Bonnefoi, Johnny Wakim, Yassine El Lamti

IEEE Open Journal of the Communications Society

Received XX Month, XXXX; revised XX Month, XXXX; accepted XX Month, XXXX; Date of publication XX Month, XXXX; date of current version XX Month, XXXX.

Digital Object Identifier 10.1109/OJCOMS.2022.1234567

When Asymmetry Helps: Joint Power and Blocklength Optimization for Non-Orthogonal Multiple Access in Downlink Communications

Haïfa Farès*, Member, IEEE, Rémi Bonnefoi†, Johnny Wakim*, and Yassine El Lamti *

[1]IETR - UMR CNRS 6164, CentraleSupélec, avenue de la Boulaie - CS 47601 35576 CESSON-SEVIGNE Cedex, France
[2]Joulwatt Technology France, Ramonville-Saint-Agne, Occitanie

CORRESPONDING AUTHOR: Haïfa Farès (e-mail: haifa.fares@centralesupelec.fr).

ABSTRACT This paper investigates downlink non-orthogonal multiple access (NOMA) in short-packet communications, specifically focusing on a scenario where an Access Point (AP) serves two users with varying channel conditions. The study explores the finite blocklength regime in order to support low latency scenarios. In this context, the conventional Shannon's capacity theorem becomes inadequate due to the non-negligible decoding error probability, resulting from finite blocklengths that do not approach infinity, which is the case of the asymptotic regime of the capacity theorem. NOMA has great potential to improve spectral efficiency compared to orthogonal multiple access by adapting power allocation to take benefit from the asymmetrical channel conditions between served users. In this study, we take the concept further by suggesting that, in the finite blocklength regime, the user with the worst communication channel can benefit from a longer blocklength. The approach considers both power and blocklength partitioning as the degrees of freedom to be tuned to enhance overall system performance. In particular, we derive the maximum achievable rates of both users when different blocklengths are assumed. We are evaluating the impact of promoting the user with the worst channel condition not only through higher power but also through a longer block on its maximum achievable rate while ensuring a minimum achievable rate for the other user. Numerical results of the exact resolution are provided. The comparative analysis of the proposed scheme with the conventional one where both users have the same blocklength shows that the asymmetry of blocklengths is as beneficial as the asymmetry in power. This observation has been verified by the achievable rate region analysis, using *Pareto Frontier* and genetic algorithm tools.

INDEX TERMS Non-Orthogonal Multiple Access (NOMA), finite blocklength, optimization, 5G, Low latency, mission-critical IoT.

I. Introduction

NOn-orthogonal multiple access (NOMA) has emerged as a promising technique in future wireless communication systems, aiming to enhance spectral efficiency and accommodate massive connectivity [1, 2]. By enabling multiple users to share the same time-frequency-code resource blocks, NOMA achieves higher spectral efficiency compared to traditional orthogonal multiple access schemes. The underlying principle of NOMA lies in the power domain, where users with varying channel conditions are assigned different power levels to ensure reliable communication. Previous research has demonstrated that the benefits of non-orthogonal access compared to orthogonal access (OMA) increase as the channel conditions of served users become more asymmetric. These studies have highlighted the potential of NOMA in improving capacity and promoting user fairness, making it an advantageous solution for enhancing the performance of 5G communications [3, 4]. In particular, NOMA offers great potential to meet massive connectivity requirements for mission-critical Internet-of-Things (IoT) applications. However, most existing works in this field have made assumptions under idealized conditions, such as asymptotic blocklength [5, 6, 7, 8, 9]. These assumptions do not align with the stringent low-latency requirements of practical systems, and they overlook an important degree of freedom, namely the blocklength, which offers additional optimization potential alongside power allocation. In this sense, it is natural to integrate the short-packet through the finite blocklength regime and NOMA techniques to achieve latency requirements [10, 11, 12]. In practical wireless

systems, the finite blocklength raises new challenges that need to be addressed for accurate performance analysis since Shannon's capacity formula is no longer applicable as the law of large numbers is not valid. However, almost all existing studies typically consider the same blocklength for all users, which is suboptimal for system optimization as it fails to leverage all available parameters for refining system design. In contrast, few recent studies have explored the variable blocklength approach, allowing different users to have distinct blocklengths [13, 14, 15]. For instance, in [13], authors demonstrate the superior performance of NOMA in reducing transmission latency regarding OMA techniques. Under certain assumptions, they find that the optimal power allocation can be solved under the condition of a common minimum blocklength for both served users. Besides, in [14], authors consider different blocklength only when they assume a cooperative NOMA scheme, where the whole blocklength is divided into two inequal phases: the broadcast phase and the relay phase. In [15], Nikbakht *et al.* derive tradeoffs between error probability, message set size, and the (finite) number of channel uses for joint channel coding of two consecutive messages with heterogeneous decoding deadlines. Their study assumes different blocklengths for consecutive arriving packets.

However, none of these previous studies have considered different blocklengths across users as an additional parameter to be considered and optimized to enhance system performance, notably in terms of maximum achievable rates.

Therefore, in our study, we propose a novel approach that extends the concept of asymmetric power allocation to incorporate asymmetric coding schemes as well. We hypothesize that in the finite blocklength regime, the user with the worst channel conditions can benefit from a longer blocklength. By appropriately partitioning both power and code resources, we aim to enhance overall system performance by maximizing the achievable rate for the user with the worst channel conditions while ensuring a minimum achievable rate for the other user. To evaluate the effectiveness of our proposed approach, we derive the maximum achievable rates for both users under the assumption of different blocklengths. The impact of promoting the user with the bad channel, not only through higher power allocation but also through the use of a longer blocklength, is thoroughly analyzed. The numerical results of the exact resolution are presented to validate the performance gains achieved by our approach. These numerical results are given for different rate constraints ranging from low to high rate constraints for the strong user. Besides, high-reliability constraints related to the error probability values are assumed to be compliant with ultra-reliable applications which is relevant for typical mission-critical IoT scenarios. Furthermore, we compare our proposed scheme with the conventional NOMA approach where both users have the same blocklength. The comparative analysis highlights the benefits of considering asymmetric coding schemes, demonstrating that the asymmetry of blocklengths can be as advantageous as the asymmetry in power allocation. These findings are verified through achievable rate region analysis, providing further insights into the performance optimization of NOMA in the finite blocklength regime.

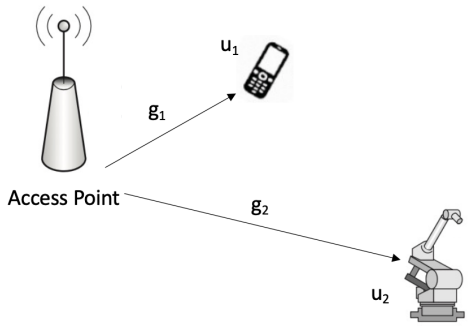

FIGURE 1: System model of interest.

The contributions of this article can be summarized as follows:

- We propose an extension of NOMA for short packets where NOMA is used and the blocklength of each packet is optimized to maximize the rate. This leads to a transmission scheme in two temporal steps. In the first phase the two packets are separated in the power domain until the end of the shorter one. In the second phase, when the first packet has been fully transmitted the base station only serves the second user.
- We express the problem of power allocation for rate maximization in the proposed scheme.
- We propose an algorithm to solve the above-mentionned problem.
- We conduct a high SINR analysis to analyze the concavity of the studied problem.
- We use numerical simulation as a means to assess the advantages of the proposed asymmetrical scheme.
- We use Pareto frontier to analyze the achievable rate regions and to confirm the advantages of the proposed scheme.

The rest of the paper is organized as follows. Section II presents the system model and formulates the optimization problem. Section III details the main guidelines to solve the optimization problem. Numerical results are presented in Section IV to draw useful insights. These results are given in terms of optimal objective function, optimal blocklength, and maximum achievable rates regions. Finally, conclusions are made in Section V.

II. System Model and Problem Formulation

This paper explores a downlink system utilizing NOMA with short packets. To address the challenges posed by strong co-channel interference and the substantial system overhead associated with user coordination, we focus on a scenario where only two users, denoted as u_1 and u_2, are paired to per-

form NOMA as depicted in Fig. 1. Without loss of generality, we consider a unique Access Point (AP) serving these two users u_1 (strong user) and u_2 (weak user) transmitting two different blocklengths m_1 and m_2, respectively. This implies that u_1 experiences superior channel conditions compared to u_2, indicated by $g_1 \geq g_2$. As a means to guarantee fairness between users, we allocate more power to the user with the worse channel gain [16]. Power allocation follows $P_1 \leq P_2$. The signal-to-noise ratios (SNRs) for users are denoted as Γ_i $(i = 1, 2)$, calculated based on

$$\Gamma_i = \frac{g_i P_i}{\sigma^2}. \tag{1}$$

Here, g_i represents the channel gain from the AP to user i, P_i denotes the power allocated to user i, and σ^2 corresponds to the noise power.

In NOMA, to improve users fairness we favor the user with worse propagation condition; we can push this reasoning even more and say that, in blocklength regime, the user who is in difficulty will also be favored by a longer blocklength. Therefore, we assume that $m_1 \leq m_2$.

According to the NOMA principle, for the weak user, Successive Interference Cancellation (SIC) is used to combat this inherent interference and we assume perfect SIC. Hence, the signal-to-interference-and-noise ratio (SINR) has to be considered and is given by

$$\Gamma_2^1 = \frac{g_2 P_2}{\sigma^2 + g_2 P_1} \tag{2}$$

Although we have not delved into signal processing techniques such as SIC, we assume that we can achieve proper detection functionality by taking some key considerations to enhance the success of SIC in NOMA:

- vital accurate knowledge of channel state information for successful SIC in NOMA, ensuring that the transmitter has up-to-date information on the channel conditions of all users.
- properly pair users with distinct channel conditions since NOMA works better when users have significantly different channel gains. This helps in achieving a better separation of signals during the SIC process.

In applications requiring ultra-reliable low-latency communication (URLLC), there is primarily an interplay among reliability, latency, and throughput, leading to tradeoffs that are closely tied to specific applications. In our study, we have chosen the example of factory automation. This particular use case is a context with low mobility and without strong bandwidth requirements, so there is no need for very high carrier frequencies, and consequently, constraints regarding delay can be relaxed, and considering quasi-static fading as a channel model is appropriate. Furthermore, note that even for massive MIMO transmission scenario, this same channel model has been emphasized as relevant for URLLC applications [17].

A. Achievable Data Rate for a Point-to-Point System

The data rate R of a communication system represents the ratio of the number of useful information bits to the number of transmitted symbols. According to Shannon's coding theorem, the Shannon capacity refers to the maximum achievable rate when an encoder/decoder pair can achieve negligible decoding error probability that tends to zero as the blocklength approaches infinity. However, in the context of URLLC applications, the blocklength for each frame is small. As a result, the decoding error probability at the receiver cannot be disregarded. In this particular context (considering a fixed short blocklength m), a more accurate expression of the maximum achievable rate has been found by Polyanskiy *et al.*[18], adopting the normal approximation:

$$R = \log_2(1 + \Gamma) - \sqrt{\frac{V(\Gamma)}{m}} \frac{Q^{-1}(\epsilon)}{\ln(2)} \tag{3}$$

where ϵ represents the target error decoding probability, $Q^{-1}(\cdot)$ is the inverse function of $Q(x) = \frac{1}{\sqrt{2\pi}} \int_x^\infty e^{-\frac{t^2}{2}} dt$, and the channel dispersion V is given by $V(\Gamma) = 1 - \frac{1}{(1+\Gamma)^2}$.

B. Achievable Data Rate for Generalized NOMA System

In the case of a conventional NOMA transmission, both users receive messages with the same blocklength, denoted as $m_1 = m_2 = m$. Using the appropriate SNR values (SNR Γ_1 for the strong user and SINR Γ_2^1 for the weak user), the maximum achievable rates for both users can be respectively expressed as:

$$R_1^{\text{NOMA}} = \log_2(1 + \Gamma_1) - \sqrt{\frac{V(\Gamma_1)}{m}} \frac{Q^{-1}(\epsilon)}{\ln 2}, \tag{4}$$

$$R_2^{\text{NOMA}} = \log_2\left(1 + \Gamma_2^1\right) - \sqrt{\frac{V(\Gamma_2^1)}{m}} \frac{Q^{-1}(\epsilon)}{\ln 2}. \tag{5}$$

As depicted in Fig. 2, for an asymmetrical NOMA transmission with $m_2 \geq m_1$ (boosting the weak user by a longer blocklength), we observe two different behaviors. For the strong user (u_1), a conventional NOMA transmission is considered. However, for the weak user (u_2), a combination of two transmission schemes is employed:

- Up to m_1, NOMA transmission is utilized (all symbols of u_1 are totally overlapping with the first m_1 symbols of u_2).
- From $m_1 + 1$ to m_2, u_1 has no more symbols to send therefore u_2 is allocated all the resources, meaning it transmits alone. Consequently, besides the longer blocklength utilized, u_2 benefits from this interference-free transmission phase.

By assuming a two-phase transmission (over time), we can consider it as an OMA-like scheme across these two phases. However, during the first phase, NOMA scheme has to be considered between users. Consequently, the maximum achievable rates for both users are given by:

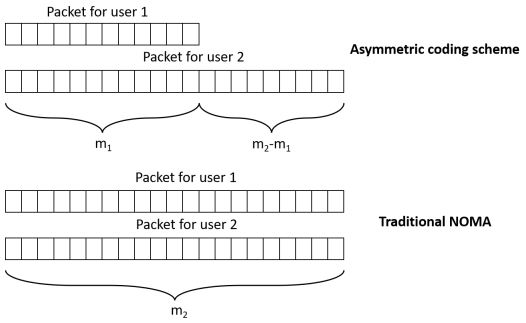

FIGURE 2: Comparison between conventional NOMA and the proposed asymmetrical scheme where the blocklength is adjusted based on the channel gain of the users.

$$R_1 = \frac{m_1}{m_2}\left(\log_2\left(1+\Gamma_1\right) - \sqrt{\frac{V(\Gamma_1)}{m_1}}\frac{Q^{-1}(\epsilon)}{\ln 2}\right), \tag{6}$$

and

$$R_2 = \underbrace{\frac{m_1}{m_2}\left(\log_2\left(1+\Gamma_2^1\right) - \sqrt{\frac{V(\Gamma_2^1)}{m_1}}\frac{Q^{-1}(\epsilon)}{\ln 2}\right)}_{m_1 \text{ symbols of both users are overlapping}} + \underbrace{\left(1-\frac{m_1}{m_2}\right)\left(\log_2\left(1+\Gamma_2\right) - \sqrt{\frac{V(\Gamma_2)}{m_2-m_1}}\frac{Q^{-1}(\epsilon)}{\ln 2}\right)}_{\text{interference-free transmission}}.$$

C. Optimization Problem Fromulation

The objective is to optimize the achievable rate of the second user, denoted as R_2, with respect to the blocklength m_1 and the allocated powers P_1 and P_2. This optimization is performed under the constraints of a fixed maximum blocklength m_2, a fixed target error decoding probability ϵ, a power budget P, and a minimum required achievable rate target for the first user, denoted as R_0. The rate constraint on the first user is important as it strikes a balance between the system rate and user fairness: maximizing the rate of the user with the lower channel gain while guaranteeing a certain rate target for the other user. The optimization problem can be formulated as follows:

$$\max_{m_1,P_1,P_2} R_2, \tag{7}$$
$$\text{s.t.} \quad m_1P_1 + m_2P_2 \le m_2P, \tag{8}$$
$$R_1 \ge R_0, \tag{9}$$
$$m_1 \le m_2. \tag{10}$$

It is worth noting that in the case of a conventional NOMA system where $m_1 = m_2 = m$, the power constraint becomes $P_1 + P_2 \le P$. Therefore, the conventional NOMA system can be considered as a specific case of this generalized NOMA system. On the other hand, for a pure time-division multiple access (TDMA) system where $m_1 + m_2 = m$, the power constraint is always $m_1P_1 + m_2P_2 \le mP$, but this implies $m_1P_1 + (m-m_1)P_2 \le mP$. The power constraint in our formulation can be justified by considering the power allocation for both NOMA and OMA transmission schemes. We can express it as:

$$\underbrace{\underbrace{m_1(P_1+P_2)}_{NOMA} + (m_2-m_1)P_2}_{OMA} \le m_2P. \tag{11}$$

To simplify the notation, we introduce $\alpha = \frac{m_1}{m_2}$.

Using this notation, the optimization problem can be rewritten as:

$$\max_{\alpha,P_1,P_2} R_2, \tag{12}$$
$$\text{s.t.} \quad \alpha P_1 + P_2 \le P, \tag{13}$$
$$R_1 \ge R_0, \tag{14}$$
$$\alpha \le 1. \tag{15}$$

III. Mathematical Resolution Guidelines

In this section, we focus on the design of the transmission rate of u_2 and joint power and blocklength allocation in this asymmetric NOMA transmission, i.e., focus on solving the optimization problem given in (12). In pursuit of this objective, our initial focus is to conduct an analysis to gain a comprehensive understanding of the constraints. Subsequently, we proceed to identify the optimal solution based on the insights obtained. Furthermore, an asymptotic analysis at a high-SNR regime is carried out.

A. Equalities in the contraints

To simplify the constraint presented in (13), we begin by studying the relationship between the maximum achievable rates, as defined in (6), and the corresponding SNR/SINR (which is directly connected to the power levels), in order to determine the monotonicity of this objective function of our optimization problem with respect to these variables.

The functions R_1 and R_2 represent the sum of elementary functions in the form of:

$$f(\Gamma, n, \epsilon) = \log_2\left(1+\Gamma\right) - K\sqrt{1-\frac{1}{(1+\Gamma)^2}}, \tag{16}$$

with

$$K = \frac{Q^{-1}(\epsilon)}{\ln 2\sqrt{n}}. \tag{17}$$

For instance, R_1 and R_2 involve $f(\Gamma)$ with different values of SNR/SINR and different blocklengths n, i.e., $\Gamma = \Gamma_1, \Gamma_2$, or Γ_2^1, and $n = \alpha m_2$ or $(1-\alpha)m_2$.

To study the variations of R_2 with respect to the power, it suffices to study that of f with respect to Γ. Therefore, for $K \ge 0$ and $\Gamma \ge 0$, we give hereafter, the derivative of $f(\Gamma)$ with respect of Γ:

$$\frac{\partial f}{\partial \Gamma} = \frac{1}{\ln(2)}\frac{1}{1+\Gamma} - \frac{K}{(1+\Gamma)^2\sqrt{\Gamma(\Gamma+2)}} \tag{18}$$

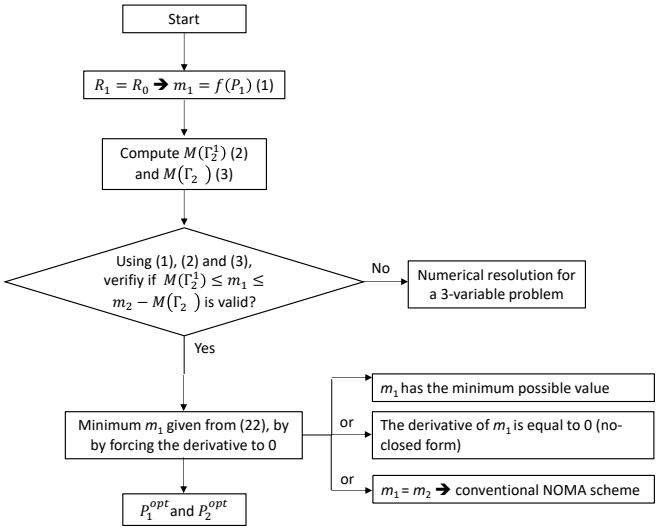

FIGURE 3: Flowchart of the algorithm for the optimization problem resolution.

The analysis of the partial derivative of f versus Γ shows that for low values of $\Gamma \geq 0$, f is a negative and decreasing function which is minimum when

$$n = \frac{\left[Q^{-1}(\epsilon)\right]^2}{\Gamma(\Gamma+1)^2(\Gamma+2)}. \tag{19}$$

Then f becomes an increasing function of Γ and becomes positive for

$$n \geq \frac{\left[Q^{-1}(\epsilon)\right]^2}{\log^2(1+\Gamma)} \frac{\left[(1+\Gamma)^2-1\right]}{(1+\Gamma)^2} = M(\Gamma). \tag{20}$$

When this condition is not met, n is too small to serve the user. In contrast, under this condition, R_2 is a positive and increasing function with respect to Γ (function of powers) and, consequently, we can set the power constraint given in equation (13) to equality when m_1 satisfies the following condition:

$$M(\Gamma_2^1) \leq m_1 \leq m2 - M(\Gamma_2). \tag{21}$$

Moreover, the equality in the maximum achievable rate constraint for u_1 (14) is always guaranteed, i.e., $R_1 = R_0$, to maximize R_2 subject to $R_1 \geq R_0$.

B. Optimal Transmission Scheme Design

Based on the previous analysis, in this subsection, we establish the optimal solution for the optimization problem stated in (12).

The resolution of the optimization problem relies on a key point that leads to two directions. The crucial aspect is to identify the conditions under which we can bound the constraints. Depending on our position relative to these conditions, we have two possible directions with very different resolution complexities:

1) Bounding the constraints. This brings us back to a single-variable problem. Once the resolution is complete, the solution (P_1^{opt}) is injected into the constraint equalities to recover the other variables (m_1^{opt} and P_2^{opt}).
2) Not bounding the constraints. This leads us to a 3-variable optimization problem to be numerically solved.

Hence, the resolution of our optimization problem follows these steps:

- **Step 1:** From the constraint $R_1 = R_0$, and assuming a fixed value for m_2, we determine the one-to-one relationship between the transmit power P_1 and coding blocklength m_1 allocated to u_1. This equality yields to 2 different possible values. If we consider the bounding expressed in (21) and only positive values for m_1, we can discriminate one possibility and only consider one unique solution.

$$\begin{aligned} m_1 = & \frac{\left[V(\Gamma_1)\left(Q^{-1}(\epsilon)\right)^2\right.}{2\ln(1+\Gamma_1)^2} + \frac{m_2 R_0}{\ln(1+\Gamma_1)} \\ & \pm \frac{\sqrt{V(\Gamma_1)}Q^{-1}(\epsilon)}{2\ln(1+\Gamma_1)^2} \\ & \sqrt{V(\Gamma_1)\left(Q^{-1}(\epsilon)\right)^2 + 4m_2 R_0 \ln(1+\Gamma_1)} \end{aligned} \tag{22}$$

  For a fixed value of m_2 and as Γ_1 is a function of the power level P_1, the coding blocklength of u_1 is then depending uniquely on its corresponding transmission power P_1.
- **Step 2:** When we satisfy the bounding of m_1 expressed in (21), we can saturate the power constraint, resulting in $P_2 = P - (m_1/m_2) * P_1$. P2 is indeed a variable in the problem; but it is worth noting that to achieve the optimal solution, the sum of P_1 and P_2 must equal P, as having more power is always profitable in terms of the system rate. Within this bounding, if we use the expression of m_1 given in (22), we establish
  - on one hand, a direct relationship between P_2 and P_1.
  - on the other hand, an equivalent bounding as that given in (21) but involving only P_1, which leads to a feasible region for P_1.
- **Step 3:** Using previous results, the studied problem becomes a one-variable optimization problem depending only on P_1 for a given feasible region. Hence, we obtain the optimal power allocation for u_1, P_1^{opt}.
- **Step 4:** Using the optimal power allocation previously obtained into the expression of the block portion of u_1 given in (22), we deduce m_1^{opt}. Likewise, using the binding power constraint we consequently obtain P_2^{opt}.

Consequently, if we are in the specific region given by (21), the problem is transformed into a single-variable problem, and we have three candidates for the optimum:

(a) the point for the minimum m_1, this occurrence is quite rare, we have the expression for the minimum m_1, and we can deduce the corresponding P_1; (b) the point when the derivative is null: in this case, the result cannot be expressed by a closed form; (c) $m_1 = m_2$, and in this case, the optimum can be expressed as it is the conventional NOMA scheme. However, if we are outside this specific region given by (21), this step-by-step resolution is no longer valid and we have to solve the optimization problem given in (12), by jointly considering power partitioning P_1, P_2 and block design m_1. The corresponding flowgraph of the algorithm for the optimization problem resolution is given by Fig. 3.

C. High-SNR Regime Analysis

In this part of the study, we can propose high SNR approximations using Taylor's expansions. We can use Taylor's expansion of the logarithm and of power functions to derive approximations for the rate of the users. To reduce the complexity of equations, we use the natural logarithm for the rate expression. For high values of the SINR Γ, using the Bachmann-Landau Little-o notation, we derive:

$$\log(1+\Gamma) = \log(\Gamma) + \left[\frac{1}{\Gamma} - \frac{1}{2(\Gamma)^2} + o\left(\frac{1}{(\Gamma)^2}\right)\right]. \quad (23)$$

Likewise, we obtain:

$$(\Gamma+1)^{-2} = (\Gamma)^{-2}\left(1+\frac{1}{\Gamma}\right)^{-2} \quad (24)$$

$$= \frac{1}{(\Gamma)^2} + o\left(\frac{1}{(\Gamma)^2}\right). \quad (25)$$

Using above-mentioned equation combined with Taylor's expansion of the square root, we derive:

$$\begin{aligned}\sqrt{V(\Gamma)} &= \sqrt{1-\frac{1}{(1+\Gamma)^2}} \\ &= \sqrt{1-\left[\frac{1}{(\Gamma)^2} + o\left(\frac{1}{(\Gamma)^2}\right)\right]} \\ &= 1 - \frac{1}{2(\Gamma)^2} + o\left(\frac{1}{(\Gamma)^2}\right). \end{aligned} \quad (26)$$

Using these two Taylor's expansions allows us to provide an order 0 approximation for the rate:

$$R(\Gamma, n, \epsilon) \approx \log(\Gamma) - \frac{Q^{-1}(\epsilon)}{\sqrt{n}}. \quad (27)$$

This approximation is illustrated in Fig. 4. The approximation is very precise when $\Gamma \geq 10dB$.

Assuming a high SNR regime, *i.e.* $\Gamma_2^1 >> 1$, $\Gamma_1 >> 1$ and $\Gamma_2 >> 1$ we approximate the rate of u_2

$$\begin{aligned}R_2 \approx \frac{1}{m2}\big(&m_1 \log(\Gamma_2^1) - Q^{-1}(\epsilon)\sqrt{m_1} \\ &+(m_2-m_1)\log(\Gamma_2) - Q^{-1}(\epsilon)\sqrt{m_2-m_1}\big). \end{aligned} \quad (28)$$

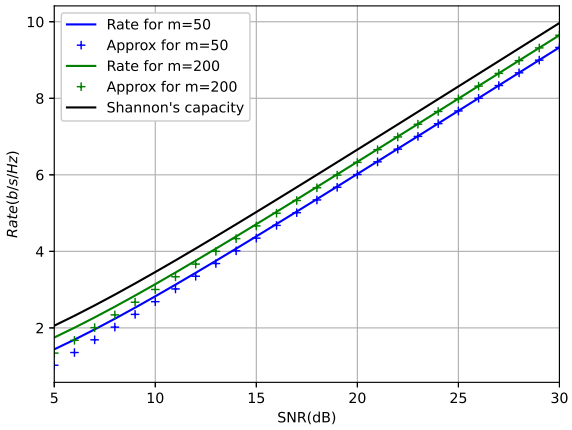

FIGURE 4: Evaluation of the proposed approximation for the rate for $\epsilon = 10^{-5}$ and for $m = 50$ and $m = 200$.

Substituting the expressions for SINR and SNR, we obtain:

$$\begin{aligned}R_2 \approx \frac{1}{m2}\Bigg(&m_1 \log\left(\frac{P_2 g_2}{\sigma^2 + P_1 g_2}\right) - Q^{-1}(\epsilon)\sqrt{m_1} \\ &+(m_2-m_1)\log\left(\frac{P_2 g_2}{\sigma^2}\right) - Q^{-1}(\epsilon)\sqrt{m_2-m_1}\Bigg). \end{aligned} \quad (29)$$

We can rephrase this approximation as

$$\begin{aligned}R_2 = \frac{1}{m2}\Big(&-m_1\log\left(1+\frac{P_1 g_2}{\sigma^2}\right) + m_2\log\left(\frac{g_2}{\sigma^2}\right) + \log(P_2) \\ &-Q^{-1}(\epsilon)\left(\sqrt{m_1}+\sqrt{m_2-m_1}\right)\Big). \end{aligned} \quad (30)$$

In the context of studying the maximum of the function, we do not take into account the constant parts of the approximation. In other words, the argument maximum of $\arg\max R_2$ expressed as

$$\begin{aligned}\arg\max\ m2\log\left(1-\frac{m_1 P_1}{m_2 P}\right) &- m_1\log\left(1+\frac{P_1 g_2}{\sigma^2}\right) \\ &- Q^{-1}(\epsilon)\left(\sqrt{m_1}+\sqrt{m_2-m_1}\right). \end{aligned} \quad (31)$$

As all the power is allocated for the users, in this expression we replaced P_2 with

$$P_2 = 1 - \frac{m_1 P_1}{m_2 P}. \quad (32)$$

The resulting expression comprises three terms

$$\begin{cases} a_1 = m2\log\left(1-\frac{m_1 P_1}{m_2 P}\right) \\ a_2 = -m_1\log\left(1+\frac{P_1 g_2}{\sigma^2}\right) \\ a_3 = -Q^{-1}(\epsilon)\left(\sqrt{m_1}+\sqrt{m_2-m_1}\right). \end{cases} \quad (33)$$

It is worth noting that $a_1 + a_2$ represents the high SINR rate approximation that user 2 would have if it could be approximated using Shannon's capacity formula.

By employing the same high SINR approximation for the rate of user 1, we derive a bijective link between P_1 and m_1

$$P_1 = \frac{\sigma^2}{g_1} e^{\frac{m_2}{m_1}\tilde{R}_0 + \frac{Q^{-1}(\epsilon)}{\sqrt{m_1}}}, \tag{34}$$

where $\tilde{R}_0 = R_0 \log(2)$ With this expression, P_1 is a positive and decreasing function of m_1. The derivative of P_1 as expressed in (34) is

$$P_1' = -\frac{\sigma^2}{g_1}\frac{1}{m_1}\left[\frac{m_2}{m_1}\tilde{R}_0 + \frac{Q^{-1}(\epsilon)}{2\sqrt{m_1}}\right] P_1. \tag{35}$$

In the following, we use the above-derived expression to study the concavity of the function defined in (31). We proceed step by step and analyze sequentially a_1, a_2 and a_3.

Lemma 1. *Assuming a rate constraint above $R_0 > \frac{1}{\log(2)}$ bits/s/Hz, a_1 is a concave function.*

Proof:

$$a_1' = \frac{P_1/P}{1 - \frac{m_1 P_1}{m_2 P}}\left[\frac{m_2}{m_1}\tilde{R}_0 + \frac{Q^{-1}(\epsilon)}{2\sqrt{m_1}} - 1\right]. \tag{36}$$

Assuming a reasonable rate constraint, i.e. higher than $\frac{1}{\log(2)}$ bits/s/Hz, the term within the parentheses is a positive and decreasing function of m_1.

Similarly, as $\tilde{R}_0 > 1$, $m_1 P_1$ is a positive and decreasing function of m_1.

$\frac{1}{1-\frac{m_1 P_1}{m_2 P}}$ is a positive and decreasing function of m_1 as the composition of an increasing and a decreasing function.

Finally, P_1/P is positive and decreasing.

As a consequence, a_1' is positive and decreasing as the product of positive and decreasing functions. So a_1 is concave. ∎

In the second step, we analyze the concavity of a_2. We derive

$$a_2'' = \frac{1}{m_1}\frac{\frac{P_1 g_2}{\sigma^2}}{1 + \frac{P_1 g_2}{\sigma^2}}\left(\frac{Q^{-1}(\epsilon)}{4\sqrt{m_1}} - \frac{1}{1 + \frac{P_1 g_2}{\sigma^2}}\left[\frac{\tilde{R}_0 m_2}{m_1} + \frac{Q^{-1}(\epsilon)}{2\sqrt{m_1}}\right]^2\right). \tag{37}$$

a_2 is concave if and only if $a_2'' \leq 0$. The concavity condition of a_2 yields to

$$\frac{g_2}{g_1} \leq e^{-\left[\frac{\tilde{R}_0 m_2}{m_1} + \frac{Q^{-1}(\epsilon)}{\sqrt{m_1}}\right]} \cdot \left(\frac{4\sqrt{m_1}}{Q^{-1}(\epsilon)}\left[\frac{\tilde{R}_0 m_2}{m_1} + \frac{Q^{-1}(\epsilon)}{2\sqrt{m_1}}\right]^2 - 1\right). \tag{38}$$

For each value of the ratio, $\frac{g_2}{g_1}$ there exists a value of m_1 above it the function a_2 is concave. In most practical case where NOMA is used $\frac{g_2}{g_1}$ is very low (below 0.1) and a_2 is concave for nearly all possible m_1 values (above $m_1 = \frac{m_2}{3}$). To illustrate this limit, for each value of the ratio $\frac{g_2}{g_1}$ we show in Fig. 5 the value of m_1 above which a_2 is concave.

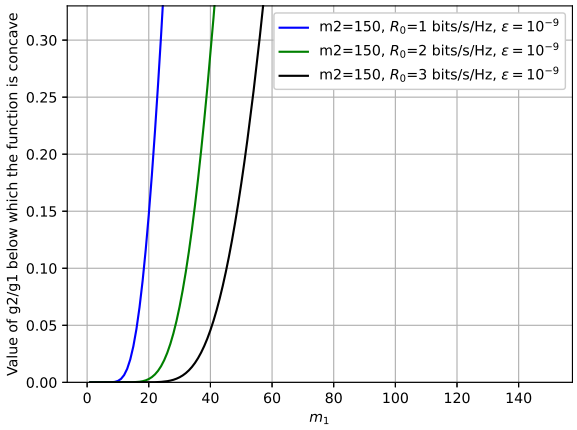

FIGURE 5: Numerical illustrations of the ratio $\frac{g_2}{g_1}$ for which the function is concave. For instance, if $\frac{g_2}{g_1} = 0.05$ the function is not concave when $m_1 = 5$ and concave when $m_1 = 45$.

In most cases a_2 is concave. So, for most values of m_1, $a_1 + a_2$, is concave as the sum of concave functions. As a consequence in a high SINR regime, if m_2 is large enough to approximate the rate of the u_2 with the Shannon's capacity formula, the function is concave and any critical point is a global maximum for the function.

Examining the second derivative of a_3 reveals that this function is convex, not concave. Specifically, when $m_1 = m_2$ the derivative of a_3 becomes infinite. When m_1 is near m_2, the derivative of the rate undergoes a steep increase, potentially indicating a global maximum.

As a conclusion of this high SINR study, the high SINR approximation for the rate of u_2 is expressed as the sum of two competing terms. The first one is almost concave and whose critical point is a maximum and the second part is whose maximum is obtained when $m_1 = m_2$, i.e. when pure NOMA is employed. So we have two candidates for the maximum the first one is the pure NOMA scheme and the other one is obtained in an asymmetrical configuration.

IV. Numerical Results and Discussion

In this section, we present numerical results to evaluate the performance of the proposed NOMA scheme when asymmetry on the power domain is extended to that on the blocklength domain. This performance is compared to the benchmark conventional NOMA scheme, taking into account finite blocklength effects. The scenario considered is of mission-critical IoT where one access point (AP) is transmitting to two different users located at different

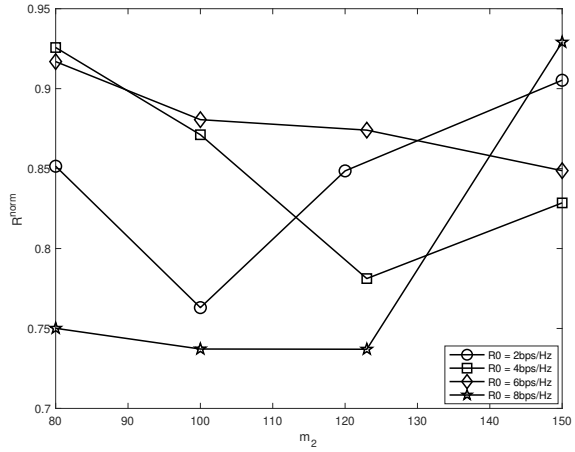

FIGURE 6: Impact of the asymmetry of the block partitioning on the maximum achievable rate of u_2: Normalized rate as a function of the maximum blocklength m_2, for a fixed target error probability $\epsilon = 10^{-9}$, a fixed available power level $P = 40$ dBm and different u_1 rate constraints R_0.

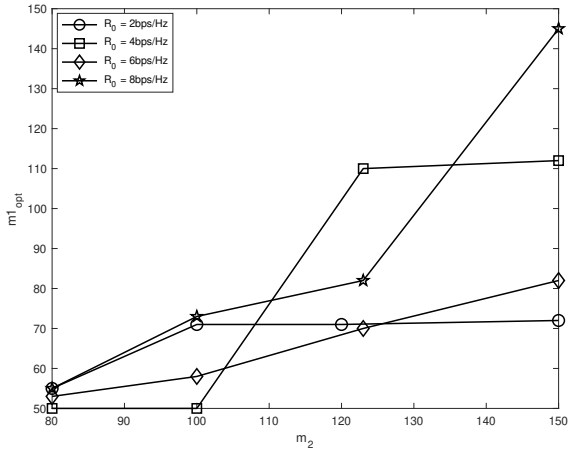

FIGURE 7: Optimal blocklength for user u_1 as a function of the fixed maximum blocklength m_2, for a fixed target error probability $\epsilon = 10^{-9}$, a fixed available power level $P = 40$ dBm and different u_1 rate constraints R_0.

distances from this common AP. We set the noise power at each user to $\sigma^2 = -114$ dBm and channel gains at u_1 and u_2 to $g_1 = 0.23{\cdot}10^{-13}$ and $g_2 = 0.56{\cdot}10^{-15}$, respectively. To have relevant values of maximum blocklengths, we express both m_1 and m_2 as a function of a fixed information length $k = 50$ and a minimum coding rate $r_{\min} = \frac{1}{3}$. Consequently, we obtain $m_1 \in [50, 150]$ and we fix $m_2 \geq m_1$ for all results discussed in this section. As shown in the numerical results in [18], the finite-blocklength approximation of the maximum achievable rate given in (3) is very accurate when the blocklength is larger than 50, which is the value of k chosen for our simulations. Furthermore, to meet the low latency requirement of the considered use case of mission-critical IoT, the minimum coding rate used to define maximum blocklength is set to a moderate value $r_{\min} = \frac{1}{3}$. Likewise, to have coherent simulation assumptions with the use case, for all results presented here, we fix the target error probability to $\epsilon = 10^{-9}$, which is a URLLC requirement.

A. Results of Optimization Problem Resolution

In order to demonstrate the beneficial effect of the blocklengths asymmetry among the users, we start by quantifying the contribution of this joint optimization of power and block allocations for this generalized NOMA transmission, compared to the reference scheme of conventional NOMA transmission where optimization efforts are focused uniquely on power allocation and an identical blocklength is deployed for both users. For instance, in Fig. 6, we illustrate the normalized optimal maximum achievable rate of u_2, which is given as the ratio between the optimal R_2 when conventional NOMA is used (i.e., $m_1 = m_2$) and optimal R_2 for the generalized NOMA (when $m_1 \leq m_2$ is used as an extra

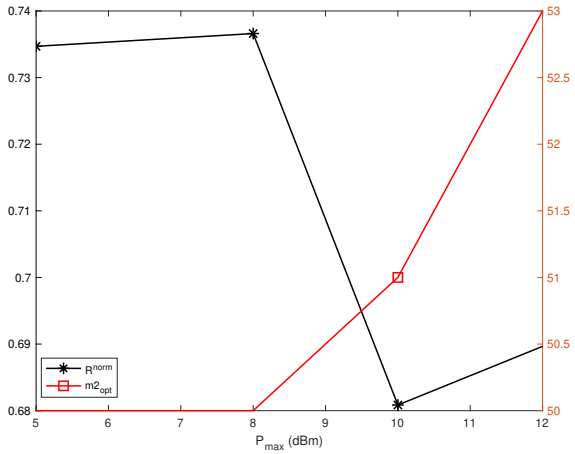

FIGURE 8: Normalized achievable rate for u_2 and its corresponding optimal blocklength for u_1 (m_1) as a function of the available power level P (at low-power regime) for a fixed maximum blocklength $m_2 = 150$, a fixed target error probability $\epsilon = 10^{-9}$ and a fixed u_1 rate constraint $R_0 = 0.5$ bits/s/Hz.

degree of freedom to optimally design the system). The normalized rate for u_2 is given versus m_2 the imposed blocklength of u_2 for different maximum rate constraints for u_1 and a given power budget. Here, we give the result for comfortable transmission conditions (an interesting interplay between the total power available and the required maximum rate constraint for u_1).

First, we observe that the asymmetric scheme is consistently advantageous under all tested conditions of different maximum blocklengths and different rate constraints.

Second, we notice that there is an optimum in terms of the maximum blocklength, providing the most significant gain by leveraging this asymmetric scheme. This optimum varies for different tested rate constraints (R_0). For instance, the best normalized achievable rate for u_2 over all configurations tested in Fig. 6 is achieved for $m_2 = 123$ and $R_0 = 8$ bits/s/Hz.

Regarding the optimal power allocation leading to these results, the main observation is that more power is assigned to the user when a shorter blocklength is chosen (the values of optimal m_1 are given later in Fig. 7). This observation proves that this general optimization considering both power allocation and code partitioning is increasing degrees of freedom in our system; and consequently offering more tunable designs.

Consequently, we can conclude that we have a great interest in refining our design by expanding the optimization from the power domain to the blocklength domain even if the conditions are not critical (high available power).

The concept of normalized rate (used in Fig. 6) was introduced to quantify performance improvements with the proposed scheme. However, it does not allow us to quantify the degree of the asymmetry to be defined for this pair of users, which is the sizing of the blocklength at u_1 that enables achieving the optimal value of maximum achievable rate at u_2. Therefore, in Fig. 7, we illustrate one of the main outcomes of the resolution of the optimization problem. In particular, we give in Fig. 7 the obtained block partitioning for u_1 versus maximum imposed blocklength m_2, for different u_1 rate constraints.

Non-surprisingly, we can see that u_1 optimal blocklength is increasing with increasing maximum imposed blocklength m_2. This implies that more redundancy can be allocated to u_1 when the whole blocklength is longer. In addition to that, for different rate constraints demanded by u_1, the optimal blocklength is not increasing with the same amount. This observation can be explained by the fact that the rates of the two users, u_1 and u_2, are conflicting, and no extreme optimum is possible for both. It is only about finding the best possible tradeoffs. Furthermore, Fig. 7 demonstrates that the highest normalized rate achieved for u_2 with a blocklength of 123 and a rate constraint for u_1 $R_0 = 8$ bits/s/Hz is made possible by employing at u_1 a blocklength $m_1 = 82$.

Finally, in order to have a more comprehensive understanding of the results from our optimization problem resolution, we need to illustrate the same metrics for different conditions. In the previous simulations, the results of the optimization were given in a high-power regime. In Fig. 8, we choose to give the optimal solution (in terms of the normalized rate at u_2 and its corresponding optimal blocklength used for u_1) versus the available power level when we are in the context of low-to-moderate power regime. These results are given for a very low-rate constraint for u_1 ($R_0 = 0.5$ bits/s/Hz) in order to be able to satisfy it even with a very low available power level. For instance, we observe a very

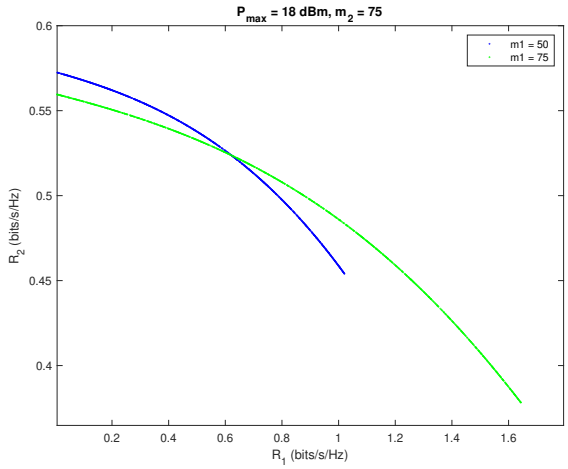

FIGURE 9: Comparison of maximum achievable rates regions for the generalized two-user NOMA-based short-packet downlink transmission for fixed maximum blocklength $m_2 = 75$, a fixed target error probability $\epsilon = 10^{-9}$ a fixed available power level $P = 18$ dBm and different fixed blocklength for u_1.

slight increase in the assigned blocklength as we increase the power budget. This can be explained by the fact that with a low power budget, not transmitting a large blocklength helps to reduce the power consumption of u_1 (it will be allocated only what is needed to satisfy its rate constraint) and thus allocating more for u_2. The general trend is a high degree of asymmetry when a low power level is available to design the power partitioning between both users when operating with NOMA technique. Furthermore, we notice from the same figure more sizable gains achieved by performing asymmetrical block partitioning than that measured for the high-power regime given in Fig. 6.

B. Pareto Frontier Analysis and Maximum Achievable Rates Region

In this section, we aim to investigate the impact of the considered blocklength asymmetry assumption on aiding the user with unfavorable channel conditions by providing a longer blocklength. This not only affects the maximum achievable rate of that particular user but also influences both users' rates since they are constrained to share the channel and collaborate in system design. To tackle this multi-objective optimization problem involving conflicting objective functions for the considered parameters, we will employ a highly suitable tool known as the *Pareto Frontier* [19, 20], a tool that we used successfully before for another context of optimization [21]. The *Pareto Frontier* allows us to illustrate the best possible trade-offs in terms of rates for both users. Subsequently, this will enable us to illustrate the regions of maximum achievable rates, which is not a common performance evaluation performed in the finite

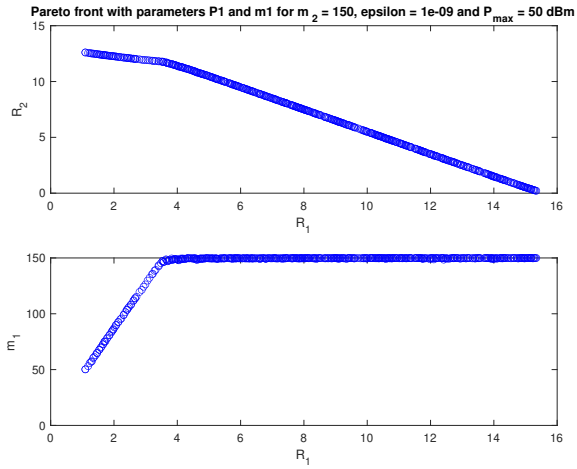

FIGURE 10: Optimal maximum achievable rates region and its corresponding optimal block partitioning for the generalized two-user NOMA-based short-packet downlink transmission for fixed maximum blocklength $m_2 = 150$, a fixed target error probability $\epsilon = 10^{-9}$ and a fixed available power level $P = 50$ dBm.

blocklength regime. Very few studies use this illustration to evaluate the whole system performance in this particular non-asymptotic context [22].

This multi-objective optimization is performed numerically using the *genetic algorithm* (GA) [23, 24]. The GA is a powerful optimization technique inspired by the process of natural selection and genetics. It is widely used to solve complex optimization problems where traditional methods may be inefficient or infeasible. By mimicking the principles of evolution, the genetic algorithm iteratively searches for the optimal solution within a population of potential solutions.

The genetic algorithm has been successfully applied in various domains, including engineering, computer science, finance, and biology. Its ability to explore vast solution spaces, handle complex constraints, and adapt to changing environments makes it a versatile and robust optimization tool.

In Fig. 9, we plot *Pareto Frontiers* on maximum achievable rates for both users u_1 and u_2 when imposing a fixed blocklength for user u_1 ($m_1 < m_2$). The *Pareto Frontier* for conventional NOMA scheme with $m_1 = m_2$ is given as a reference benchmark.

First, We can verify the general trend of performance improvement in asymmetric NOMA scheme when reducing the blocklength relative to u_1 below a certain achievable rate for u_1. Here, we are offering better achievable rates for u_2, when the achievable rate of u_1 $R_1 \leq 0.6$ bits/s/Hz. Let us recall that we are not in the context of a high-power regime.

Now, in Fig. 10, we plot the *Pareto Frontier* on maximum achievable rates for variable u_1 blocklength m_1 allowing better refining of the system design, as well as the corresponding optimal value of m_1. We start by highlighting that we are evaluating the system in a high-power regime. We can see that this more tunable design achieves the performance of the conventional NOMA scheme when it is performing better, i.e., when we are at a high-rate regime for u_1. The corresponding optimal blocklength allocation for this context is generally equal to or slightly less than the maximum blocklength, used at the side of u_2. For low to moderate-rate regime for u_1, we notice that the slopes of the curves illustrating $R_2(R_1)$ and $m_1(R_1)$ are opposite. This translates to the fact that when low rates are achieved for u_1, short blocklengths are needed in terms of m_1, subsequently leading to an increase in R_2 compared to conventional NOMA scheme ($m_1 = m_2$).

V. Conclusion

In conclusion, this paper explores the finite blocklength regime for a downlink NOMA transmission for two users to support low-latency requirements. To address this, the study proposes utilizing a longer blocklength to benefit the user experiencing difficulty due to bad channel conditions. Both power and block partitioning are considered as degrees of freedom to enhance overall system performance. The proposed NOMA scheme with asymmetry in both power and block domains has been evaluated and compared to the benchmark conventional NOMA scheme, considering finite blocklength effects. The performance analysis was conducted in the context of mission-critical IoT, where one access point transmits to two users located at different distances. The results showed the beneficial effect of blocklength asymmetry, where the joint optimization of power and blocklength allocations outperformed the conventional NOMA scheme. The trade-off between the rate constraint for the first user and the power budget was explored, demonstrating that lower power budgets lead to greater improvements with the proposed scheme. Furthermore, the optimal blocklength allocation for the first user was investigated, showing a slight increase in blocklength as the power budget increased (when we are operating in a low-power regime). Finally, the use of a Pareto Frontier and a genetic algorithm was introduced as a suitable tool for resolving the multi-objective optimization problem, providing insights into the trade-offs between the achievable rates for both users in the asymmetric NOMA scheme.

In our future work, we will extend the results obtained in this article. The first approach is to adapt the transmit power of user 2 for each of the two transmission phases to emphasize the benefits of the asymmetrical NOMA. A second solution lies in extending the proposed approach to Rate Splitting Multiple Access (RSMA) which has already been proposed for short packet transmissions [25].

REFERENCES

[1] S. Timotheou and I. Krikidis, "Fairness for non-orthogonal multiple access in 5G systems," *IEEE Sig-*

nal Process. Lett., vol. 22, no. 10, p. 1647–1651, 2015.

[2] X. Chen, Z. Zhang, C. Zhong, R. Jia, and D. Ng, "Fully non-orthogonal communication for massive access," *IEEE Transactions on Communications*, vol. 66, no. 4, p. 1717–1731, 2018.

[3] S.Islam, N. Avazov, O. Dobre, and K. Kwak, "Power-domain non-orthogonal multiple access (NOMA) in 5g systems: Potential and challenges," *IEEE Commun. Surv. Tut.*, vol. 105, no. 12, p. 2347–2381, 2017.

[4] Y. Liu, Z. Qin, M. Elkashlan, Z. Ding, A. Nallanathan, and L. Hanzo, "Non-orthogonal multiple access for 5G and beyond," vol. 19, no. 2. Proc. IEEE, 2017, pp. 721–742.

[5] G. Gui, H. Sari, and E. Biglieri, "A new definition of fairness for non-orthogonal multiple access," *IEEE Communications Letters*, vol. 23, no. 7, pp. 1267–1271, 2019.

[6] P. Bélis, R. Bonnefoi, H. Farès, and Y. Louët, "Optimal power and resource allocation for transmit power minimization in OFDMA-based NOMA networks," in *2019 IEEE Wireless Communications and Networking Conference (WCNC)*, 2019, pp. 1–7.

[7] R. Bonnefoi, P. Bélis, H. Farès, and Y. Louët, "Optimal power allocation for minimizing the energy consumption of a NOMA base station with cell DTx," in *URSI Asia-Pacific Radio Science Conference (AP-RASC)*, 2019, pp. 1–7.

[8] H. Al-Obiedollah, K. Cumanan, H. B. Salameh, G. Chen, Z. Ding, and O. A. Dobre, "Downlink multi-carrier NOMA with opportunistic bandwidth allocations," *IEEE Wireless Communications Letters*, vol. 10, no. 11, pp. 2426–2429, 2021.

[9] M. Bello, W. Yu, A. Chorti, and L. Musavian, "Performance analysis of NOMA uplink networks under statistical QoS delay constraints," in *ICC 2020 - 2020 IEEE International Conference on Communications (ICC)*, 2020, pp. 1–7.

[10] X. Sun, S. Yan, N. Yang, Z. Ding, C. Shen, and Z. Zhong, "Effective capacity of noma with finite blocklength for low-latency communications," *arXiv preprint arXiv:2002.07098*, 2020.

[11] Y. Yu, H. Chen, Y. Li, Z. Ding, and B. Vucetic, "On the performance of non-orthogonal multiple access in short-packet communications," *IEEE Commun. Lett.*, vol. 22, no. 3, p. 590–593, 2018.

[12] X. Sun, S. Yan, N. Yang, Z. Ding, C. Shen, and Z. Zhong, "Shortpacket downlink transmission with non-orthogonal multiple access," *IEEE Trans. Wireless Commun.*, vol. 17, no. 7, p. 4550–4564, 2018.

[13] Y. Yu, H. Chen, Y. Li, Z. Ding, and B. Vucetic, "On the performance of non-orthogonal multiple access in short-packet communications," *IEEE Communications Letters*, vol. 22, no. 3, pp. 590–593, 2018.

[14] H. Ren, C. Pan, Y. Deng, M. Elkashlan, and A. Nallanathan, "Joint power and blocklength optimization for URLLC in a factory automation scenario," *IEEE Transactions on Wireless Communications*, vol. 19, no. 3, pp. 1786–1801, 2020.

[15] H. Nikbakht, M. Egan, and J.-M. Gorce, "Joint channel coding of consecutive messages with heterogeneous decoding deadlines in the finite blocklength regime," in *2022 IEEE Wireless Communications and Networking Conference (WCNC)*, 2022, pp. 2423–2428.

[16] M. Vaezi, R. Schober, Z. Ding, and H. V. Poor, "Non-orthogonal multiple access: Common myths and critical questions," *IEEE Wireless Communications*, vol. 26, no. 5, pp. 174–180, 2019.

[17] A. Lancho, J. Östman, G. Durisi, and L. Sanguinetti, "A finite-blocklength analysis for urllc with massive mimo," in *2021 IEEE International Conference on Communication (ICC))*, 2021.

[18] Y. Polyanskiy, H. V. Poor, and S. Verdu, "Channel coding rate in the finite blocklength regime," *IEEE Transactions on Information Theory*, vol. 56, no. 5, pp. 2307–2359, 2010.

[19] R. T. Marler and J. S. Arora, "Survey of multi-objective optimization methods for engineering," *Structural and multidisciplinary optimization*, vol. 26, no. 6, pp. 369–395, 2004.

[20] P. Ngatchou, A. Zarei, and A. El-Sharkawi, "Pareto multi objective optimization," *Proceedings of the 13th International Conference on, Intelligent Systems Application to Power Systems*, pp. 84–91, Nov 2005.

[21] K. Kassan, H. Farès, D. C. Glattli, and Y. Louët, "Performance vs. spectral properties for single-sideband continuous phase modulation," *IEEE Transactions on Communications*, vol. 69, no. 7, pp. 4402–4416, 2021.

[22] J. Xu, O. Dizdar, and B. Clerckx, "Rate-splitting multiple access for short-packet uplink communications: A finite blocklength analysis," *IEEE Communications Letters*, vol. 27, no. 2, pp. 517–521, 2023.

[23] D. E. Goldberg, *Genetic Algorithms in Search, Optimization, and Machine Learning*. Addison-Wesley Professional, 1989.

[24] J. H. Holland, *Adaptation in Natural and Artificial Systems*. MIT Press, 1992.

[25] Y. Xu, Y. Mao, O. Dizdar, and B. Clerckx, "Max-min fairness of rate-splitting multiple access with finite blocklength communications," *IEEE Transactions on Vehicular Technology*, vol. 72, no. 5, pp. 6816–6821, 2023.

Haïfa Farès received bachelor's and M.Sc. degrees in telecommunication engineering from the Higher School of Communications of Tunis (Sup'Com), in 2007 and 2008, respectively, and the Ph.D. degree in digital communications from IMT-Atlantique, France, in 2011. She is currently an Associate Professor at CentraleSupélec of Rennes. She is a member of the SIGNAL research group of the CNRS Institute of Electronics and Digital Technologies (IETR), Rennes Laboratory. Her research interests include the area of communication theory, including nonlinear modulations, green communications, iterative decoding algorithms, and non-orthogonal multiple access.

Rémi Bonnefoi received an engineering degree and a Ph.D. in Telecommunications from CentraleSupélec. He has proposed algorithms for optimizing mobile network energy consumption and reducing collisions in IoT networks. He worked for four years at Edison Ways, a French start-up and he is now a digital design engineer at Joulwatt Technology.

Johnny Wakim is an engineering student at CentraleSupelec, currently in his final year of studies. His journey began at the Lebanese University in Lebanon, where he pursued computer and communication engineering. Later, he embarked on a double diploma program with CentraleSupelec, specializing in embedded systems and IoT. As an aspiring engineer, his areas of interest encompass telecommunication technologies, A.I., and programming, with a particular focus on edge computing.

Yassine EL LAMTI is an engineering student at Ecole Centrale Casablanca in Morocco, and is pursuing his final year at CentraleSupélec in Rennes as part of an exchange program. After following a generalist program, he chose to specialize in IoT and embedded digital electronics. He is also doing a double degree diploma at INSA Rennes as part of a Master's program in complex systems engineering. Interested in new processing and communication technologies, and attracted by the industrial world, he focuses his career and projects on subjects around innovations in telecommunications and data processing and their potential gains for the fourth industrial revolution.